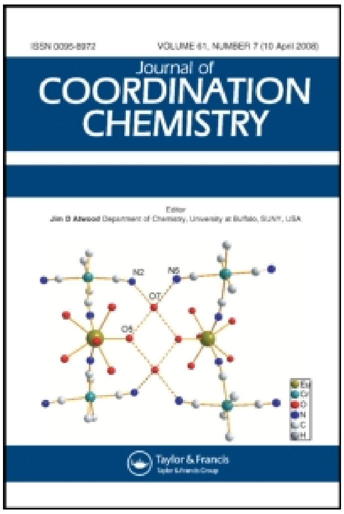

Journal of Coordination Chemistry
Publication details, including instructions for authors and subscription information:
http://www.informaworld.com/smpp/title~content=t713455674

Oxidative DNA cleavage by Cu(II) complexes of 1,10-phenanthroline-5,6-dione

Ying-Ying Kou[a]; Jin-Lei Tian[a]; Dong-Dong Li[a]; Hui Liu[a]; Wen Gu[a]; Shi-Ping Yan[a]
[a] Department of Chemistry, Nankai University, Tianjin, P.R. China

To cite this Article Kou, Ying-Ying , Tian, Jin-Lei , Li, Dong-Dong , Liu, Hui , Gu, Wen and Yan, Shi-Ping(2009) 'Oxidative DNA cleavage by Cu(II) complexes of 1,10-phenanthroline-5,6-dione', Journal of Coordination Chemistry, 62: 13, 2182 — 2192

To link to this Article: DOI: 10.1080/00958970902763271

URL: http://dx.doi.org/10.1080/00958970902763271

Journal of Coordination Chemistry
Vol. 62, No. 13, 10 July 2009, 2182–2192

Oxidative DNA cleavage by Cu(II) complexes of 1,10-phenanthroline-5,6-dione

YING-YING KOU*, JIN-LEI TIAN, DONG-DONG LI,
HUI LIU, WEN GU and SHI-PING YAN

Department of Chemistry, Nankai University, Tianjin, P.R. China

(*Received 29 August 2008; in final form 15 October 2008*)

A dimeric dichloro-bridged copper(II) complex $[Cu_2(pdon)_2Cl_4] \cdot 2DMF$ (**1**) and two mononuclear copper(II) complexes $[Cu(pdon)(DMSO)Cl_2] \cdot DMSO \cdot H_2O$ (**2**) and $[Cu(pdon)_3] \cdot (ClO_4)_2 \cdot 2.25CH_3CN \cdot 6H_2O$ (**3**) (pdon = 1,10-phenanthroline-5,6-dione) have been synthesized and characterized. Variable-temperature magnetic susceptibility studies indicate the existence of weak anti-ferromagnetic coupling in the binuclear complex. The interaction of these complexes with CT-DNA (calf thymus DNA) has been studied using absorption and emission spectral methods. The apparent binding constants (K_{app}) for **1**, **2** and **3** are 5.20×10^5, 2.68×10^5 and $7.05 \times 10^5\ M^{-1}$, respectively, showing moderate intercalative binding modes. All of these complexes cleave plasmid DNA to nicked DNA in a sequential manner as the concentration or reaction time is increased. The cleavage mechanism between the complex and plasmid DNA is likely to involve singlet oxygen $^1O_2$ and $^{\bullet}OH$ as reactive oxygen species.

Keywords: Copper(II) complexes; 1,10-Phenanthroline-5,6-dione; Crystal structure; Plasmid DNA; Oxidative DNA cleavage

1. Introduction

Over the last two decades, interactions of transition metal complexes with nucleic acids have been of interest in biochemical and coordination chemical research [1–4]. Especially copper complexes containing phenanthroline bases have received interest in development of artificial nucleases [5–9]. Cu^{II} complexes of 1,10-phenanthroline (phen), which cleave DNA duplexes [10–15], show antiviral activity upon interaction with nucleic acid templates and inhibit proviral DNA synthesis [5]. In the presence of H_2O_2 or O_2 and reducing agents, such complexes cleave DNA by cycling between $[Cu(phen)_2]^{2+}$ and $[Cu(phen)_2]^{+}$ catalyzing formation of activated oxygen species (O_2^- and $^{\bullet}OH$) [16–18]. However, the mechanism by which copper–phenanthroline complexes damage DNA is complicated, and several issues remain unresolved [19, 20]. Due to the high activity of this system, a number of small metal complexes of planar aromatic chelating ligands have been tested as DNA intercalating agents and metal-based chemical nucleases [21–23]. Many parameters, including the size, shape,

---

*Corresponding author. Email: kouyingying@mail.nankai.edu.cn

Journal of Coordination Chemistry
ISSN 0095-8972 print/ISSN 1029-0389 online
DOI: 10.1080/00958970902763271

and chirality of these compounds plus the structure and composition of the target DNA, control bonding and chemical modification [22, 24].

1,10-Phenanthroline-5,6-dione (pdon) is a redox active ligand because of the *o*-quinoid moiety at positions 5 and 6. Metal complexes with this dioxolene ligand which generate unique photochemical and electrochemical properties have been studied [25, 26] since dioxolene can take three oxidation states (quinone, semiquinone, and catecholate); as far as we know, it has not been used to study DNA bonding and cleavage activity.

In order to investigate the chemical nuclease activity of the complexes containing pdon, we have synthesized and characterized a binuclear Cu^{2+} complex (**1**) and studied its DNA cleavage activity. Comparing with the binuclear complex, the biochemical activities of two mononuclear Cu^{2+} complexes (**2** and **3**), which have been characterized by single crystal structures in our research group [27], have also been investigated. In this article, the interaction between calf thymus DNA (CT-DNA) and **1–3** were investigated by UV absorption and fluorescent spectroscopy, as well as the DNA cleavage experiments. All complexes efficiently cleave pBR322 DNA without addition of external agents, and the DNA cleavage reaction was inhibited by DMSO, NaN_3, and EDTA. These results suggest that the mechanisms of DNA cleavage by these complexes are oxidative cleavage.

2. Experimental

2.1. *Materials and instrumentation*

Ligand pdon was synthesized according to literature procedure [28]. Ethidium bromide (EB), CT-DNA and pBR322 plasmid DNA were from Sigma. *Tris*-HCl buffer (*Tris* = *tris*(hydroxymethyl)aminomethane) solution was prepared using deionized sonicated triply-distilled water. All other reagents and chemicals were purchased from commercial sources and used as received. Elemental analyses for C, H, and N were obtained on a Perkin–Elmer analyzer Model 240. Infrared spectroscopy on KBr pellets was performed on a Bruker Vector 22 FT-IR spectrophotometer from 4000–400 cm^{-1}. The electronic spectra were measured on a JASCO V-570 spectrophotometer. Fluorescence spectral data were obtained on a MPF-4 fluorescence spectrophotometer at room temperature. Variable-temperature magnetic susceptibility measurements were performed on a MPMS XL-7 SQUID with a field of 2000 Oe. Diamagnetic corrections were estimated from Pascal's constants.

2.2. *Preparation of complexes*

2.2.1. Synthesis of $[Cu_2(pdon)_2Cl_4]\cdot 2DMF$ (1). To an aqueous solution (5 mL) of $CuCl_2 \cdot 2H_2O$ (0.2 mmol, 0.034 g) was added 15 mL methanol/DMF (1 : 1) mixture of pdon (0.2 mmol) and the resulting solution was stirred overnight. The solution was filtered and green block crystals suitable for X-ray diffraction were obtained by slow evaporation of the filtrate after several days, collected by filtration, washed with diethyl ether and dried in air. Yield: 45% (based on the copper salts). Elemental analysis

Table 1. Crystal data and structure refinement for **1**.

Empirical formula	$C_{30}H_{26}Cl_4Cu_2N_6O_6$
Formula weight	835.45
Temperature (K)	293(2) K
Wavelength (Å)	0.71073
Crystal system	Triclinic
Space group	$P\bar{1}$
Units of dimensions (Å, °)	
a	8.0484(16)
b	8.5291(17)
c	12.139(2)
α	94.45(3)
β	90.47(3)
γ	105.25(3)
Volume (Å^3)	801.2(3)
Z	1
D_{Calcd} (g cm^{-3})	1.732
Absorption coefficient (mm^{-1})	1.716
F (000)	422
Crystal size (mm)	0.08 × 0.06 × 0.02
θ range (°) for data collection	2.48–27.87
Limiting indices	$-10 \le h \le 10$, $-11 \le k \le 6$, $-15 \le l \le 15$
Reflections collected/unique	6168/3757 [$R_{int} = 0.0231$]
Max. and min. transmission	0.9665/0.8749
Data/restraints/parameters	3757/0/219
Goodness of fit on F^2	0.981
Final R indices [$I > 2\sigma(I)$]	$R_1 = 0.0282$, $wR_2 = 0.0707$
R indices (all data)	$R_1 = 0.0347$, $wR_2 = 0.0728$
Largest different peak and hole (e Å^{-3})	0.525/−0.387

data: calculated for $C_{30}H_{26}Cl_4Cu_2N_6O_6$ (%): C, 43.13; H, 3.14; N, 10.06. Found (%): C, 43.15; H, 3.11; N, 10.05.

$[Cu(pdon)(DMSO)Cl_2] \cdot DMSO \cdot H_2O$ (**2**) and $[Cu(pdon)_3](ClO_4)_2 \cdot 2.25CH_3CN \cdot 6H_2O$ (**3**) were synthesized according to the literature procedure [27].

2.3. *X-ray crystallography*

Diffraction data for **1** were collected at 113(2) K with a Bruker Smart 1000 CCD diffractometer using Mo-Kα radiation ($\lambda = 0.71073$ Å) with the ω–2θ scan technique. An empirical absorption correction was applied to raw intensities [29]. The structure was solved by direct methods (SHELXS-97) and refined with full-matrix least-squares on F^2 using SHELXL-97 [30, 31]. The hydrogen atoms were added theoretically, riding on the concerned atoms and refined with fixed thermal factors. The details of crystallographic data and structure refinement parameters are summarized in table 1 (Supplementary material).

2.4. *DNA-binding and cleavage experiments*

The UV absorbances at 260 nm and 280 nm of the CT-DNA solution in 18 mM NaCl/50 mM *Tris*-HCl buffer (pH = 7.2) give a ratio of 1.8–1.9, indicating that the DNA was sufficiently free of protein [32]. The concentration of CT-DNA was determined from its absorption intensity at 260 nm with a molar extinction coefficient of 6600 M^{-1} cm^{-1} [33]. The absorption spectra of **1–3** binding to DNA were performed by increasing amount of CT-DNA to the complexes in *Tris*-HCl buffer (pH = 7.2).

The relative bindings of **1–3** to CT-DNA were studied with an EB-DNA solution in *Tris*-HCl/NaCl buffer (pH = 7.2). The fluorescence spectra were recorded at room temperature with excitation at 510 nm and emission at 602 nm. Such experiment was carried out by titrating complexes into EB-DNA solution containing 4.0×10^{-6} M of EB and 80×10^{-6} M of DNA.

The DNA cleavage experiments were done by agarose gel electrophoresis, which was performed by incubation at 37°C for 3 h as follows: pBR322DNA (0.1 µg/µL) in 50 mM *Tris*-HCl/18 mM NaCl buffer (pH = 7.2) was treated with complex in the absence of additives. The samples were incubated for 3 h and then loading buffer was added. The samples were electrophoresed for 4 h at 80 V on 0.8% agarose gel using *Tris*-boric acid–EDTA buffer (TBE). After electrophoresis, bands were visualized by UV light and photographed. Quantification of cleavage products was performed by UVIpro software, Version 10.03. Supercoiled plasmid DNA values were corrected by a factor 1.3, based on average literature estimate of lowered binding of ethidium [34].

Cleavage mechanistic investigations of pBR322 DNA were done using different reagents such as DMSO, NaN_3, SOD and EDTA added to pBR322 DNA prior to addition of complex.

Anaerobic conditions were achieved using an anmbraum LABStar glove box. Deoxygenated solutions were prepared by four freeze-pump-thaw cycles. Before each cycle the solutions were equilibrated with nitrogen to aid the deoxygenation process. The deoxygenated solutions were stored under a nitrogen atmosphere prior to use. Reaction mixtures were prepared in a glove box by addition of the appropriate volumes of stock solutions to the reaction tubes.

3. Results and discussion

3.1. *X-ray structure characterization*

The structure of **1** consists of a dimeric $[Cu(pdon)(\mu\text{-}Cl)Cl]_2$ neutral molecule and two DMF molecules. The structure of **1** is shown in figure 1 and selected bond lengths and angles are listed in table 2. In the dimeric unit, the two Cu^{II} ions are bridged symmetrically by two Cl^- with the Cu1 $\cdots$ Cu1A distance of 3.445 Å. Each Cu^{II} center is five-coordinate with a bidentate chelating pdon, two bridging Cl^- and a terminal Cl^-. According to the Addison/Reedijk geometric criterion [35], the coordination environment of the central Cu atom can be described as a distorted square pyramid reflected by the τ value of 0.11. Cu1 is 0.1756 Å above the mean basal plane defined by N1–N2–Cl1–Cl2A and Cl2 occupies the apical position. The axial Cu1–Cl2 bond length of 2.6894 Å is significantly longer than the Cu–Cl bond lengths in the basal plane (Cu1–Cl1, 2.2376 Å; Cu1–Cl2A, 2.2651 Å). An analog of **1**, $[Cu(pdon)(\mu\text{-}Cl)Cl]_2 \cdot 2CH_3CN$ was reported by Stephenson and Hardie [36] with bond lengths and angles as well as the geometry of central Cu^{II} very close to **1**. The analog crystallizes in a monoclinic cell and the structure was solved in space group *P21/n*, while **1** crystallizes in a triclinic system with $P\bar{1}$ space group. Such difference may be caused by the dissimilar solvate molecules. In this analog [36], the authors mainly discussed the structure and chemical properties

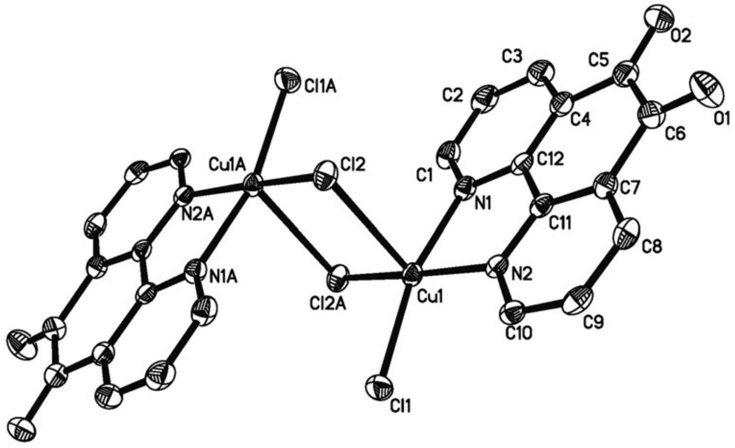

Figure 1. The labeling scheme of [$Cu_2(pdon)_2Cl_4$]; hydrogen atoms and DMF are omitted for clarity.

Table 2. Selected bond lengths (Å) and angles (°) for **1**.

Cu1–N2	2.0377(18)	Cu1–N1	2.0399(16)
Cu1–Cl1	2.2376(6)	Cu1–Cl2A	2.2651(10)
Cu1–Cl2	2.6894(9)		
N2–Cu1–N1	80.39(7)	N2–Cu1–Cl1	92.99(6)
N1–Cu1–Cl1	165.19(5)	N2–Cu1–Cl2A	172.17(4)
N1–Cu1–Cl2A	93.26(6)	Cl1–Cu1–Cl2A	92.11(4)
N2–Cu1–Cl2	91.87(5)	N1–Cu1–Cl2	86.77(5)
Cl1–Cu1–Cl2	106.80(3)	Cl2A–Cu1–Cl2	92.34(3)
Cu1–Cl2–Cu1A	87.66(3)		

were not studied. In this article, we will investigate its magnetic properties as well as chemical nuclease activities.

The X-ray crystal structures of **2** and **3** are shown in Supplementary material.

3.2. *IR spectrum*

IR spectra of **1** show two strong absorption bands: $\nu_{(C=O)}$ and $\nu_{(C=N)}$ at 1704 cm^{-1} and 1656 cm^{-1}, respectively. The peak about 1576 cm^{-1} shows the $\nu_{(C=N)}$ of DMF. All of these results were consistent with the crystal structure.

3.3. *Magnetic properties*

The variable-temperature magnetic susceptibility data for **1** were recorded from 2–300 K. The effective magnetic moment (μ_{eff}) and the molar magnetic susceptibilities (χ_M) *versus* T are plotted in figure 2. At room temperature, the effective magnetic moment is 2.69 B.M., larger than the predicted spin-only value of 2.45 B.M. for a dinuclear Cu^{II} ($S = 1/2$) unit. The μ_{eff} value decreases gradually with decreasing temperature to 2.27 B.M. at 2 K, indicating the presence of weak anti-ferromagnetic exchange interactions between the adjacent copper ions through the dichloro-bridge.

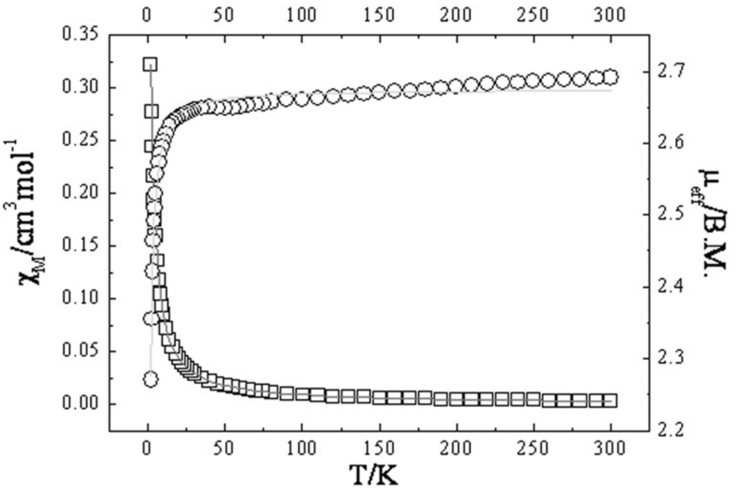

Figure 2. χ_M (□) *vs.* T and μ_{eff} (○) *vs.* T plots for **1**. Solid lines represent the best theoretical fits.

Taking into account the dimeric structure, the fit of the magnetic data was made using the expression derived from the Hamiltonian $\hat{H} = -2J\hat{S}_1 \cdot \hat{S}_2$, with J = magnetic exchange coupling constant and $S_1 = S_2 = 1/2$, while considering the intermolecular interaction. It can be theoretically modeled as equations (1) and (2):

$$\chi_M = \frac{2Ng^2\beta^2}{kT} \times \frac{1}{3 + e^{-2J/kT}} \tag{1}$$

$$\chi'_M = \frac{\chi_M}{1 - (2zJ'/Ng^2\beta^2)\chi_M} \tag{2}$$

The best fit parameters were $J = -0.58\,\text{cm}^{-1}$, $g = 2.18$ and $zJ' = -0.08\,\text{cm}^{-1}$ with the agreement factor $R = 3 \times 10^{-5}$. The negative J parameter implies a very weak intradimer anti-ferromagnetic interaction.

Complex **1** contains a [Cu(μ-Cl)$_2$Cu] core and each Cu^{II} atom has a distorted square pyramidal environment. To date, three types [37–39] of pyramidal arrangements in [Cu(μ-Cl)$_2$Cu] units are found in the literature: (i) square pyramids sharing a base-to-apex edge but with parallel basal planes; (ii) square pyramids sharing a basal edge with co-planar basal planes; (iii) square pyramids sharing one base-to-apex edge with the two bases nearly perpendicular to one another. For **1**, it belongs to the type I. Marsh *et al.* [40] have shown that the singlet–triplet gap in type I compounds varies in a regular way with the quotient φ/R, where φ is the bridging angle of Cu^{II}–Cl–Cu^{II} and R the long out-of-plane Cu^{II}–Cl bond distance. It was found that for values of this quotient lower than 32.6 and higher than 34.8, the exchange interaction is anti-ferromagnetic. For values falling between these limits, the exchange interaction was ferromagnetic. For **1**, the corresponding Cu^{II}–Cl–Cu^{II} and Cu^{II}–Cl values are 87.66 and 2.6894 Å, generating the quotient φ/R value of 32.59. Such φ/R value in **1** is almost the limit of 32.6, so the complex is not explained by Hatfield's rule and other structural factors should be taken into account. In **1**, the geometry of Cu^{II} is not a perfect square-pyramid, thus the magnetic orbital is a mixture of $d_{x^2-y^2}$ and d_{z^2}, mainly located in the equatorial plane

Table 3. Change in spectral features of the copper(II) complexes on interaction with CT-DNA in 50 mM *Tris*-HCl/18 mM NaCl buffer (pH = 7.2).

Complex	Change in absorptivity	$\lambda_{\max}$ (nm)	$\Delta\lambda_{\max}$ (nm)	$\Delta\varepsilon$ (%)
1	Hypochromism	218	8	47.37
2	Hypochromism	208	12	22.12
3	Hypochromism	208	10	27.77

($d_{x^2-y^2}$) but with non-zero spin density on its axial position. This feature (participation of the d_{z^2} orbital) creates a small overlap between the two Cu^{II} magnetic orbitals, giving the anti-ferromagnetic coupling [37–39].

3.4. *DNA binding properties*

DNA binding is the critical step for DNA cleavage in most cases. Therefore, the binding of **1**–**3** to CT-DNA was studied using UV–Vis absorption and fluorescence spectroscopy. Electronic absorption spectroscopy is one of the most useful techniques for DNA-binding studies of metal complexes. The absorption spectra of copper(II) complexes in the absence and presence of CT-DNA at different concentrations are shown in Supplementary material. The absorption peaks with maxima of 210 nm, 250 nm and 320 nm are attributed to intraligand π–π^* and n–π^* transitions, respectively. The intense ligand-based (π–π^*) absorption is used to monitor the interaction of the complexes with CT-DNA. Complexes bound to DNA through intercalation, which involves a strong stacking interaction of the planar aromatic rings of the coordinated ligand with the base pairs of DNA, usually result in hypochromism and red shift of ligand-band or charge transfer bands [41]. All the present complexes exhibit significant hypochromism (22.12–47.37%) on the incremental addition of DNA with varying red shifts (Supplementary material and table 3). The observed hypochromisms are much higher than observed for $[Cu(2,9\text{-dmp})_2]^{2+}$ (1.3%) (dmp = 2,9-dimethyl-1,10-phenanthroline) [42], which was proposed to form covalent bonds with the DNA base pairs [43]. Furthermore, as the extent of hypochromism is consistent with the strength of intercalative interaction, it is evident that the dinuclear complex **1** exhibits the best DNA binding affinity.

To further clarify the binding of complexes, fluorescence spectral measurements were carried out. The addition of complex to the DNA bound EB solutions caused obvious reduction in emission intensities, indicating that complex competitively bound to DNA with EB. The extent of reduction of the emission intensity gives a measure of the binding propensity of the complex to DNA. According to the classical Stern–Volmer equation [44] $I_0/I = 1 + K\,[Q]$; I_0 and I are the fluorescence intensities in the absence and presence of the quencher, respectively. K is a linear Stern–Volmer quenching constant. [Q] is the concentration of the quencher. The quenching plots (figure 3) illustrate that quenching of EB bound to DNA by complexes agree with the linear Stern–Volmer equation, indicating the complexes bind to DNA. In the plot of I_0/I *versus* the concentrations of complexes, K is given by the ratio of the slope to intercept. According to the equation K_{EB} [EB] = K_{app} [complex], where the complex concentration was the value at a 50% reduction of the fluorescence intensity of EB and $K_{EB} = 1.0 \times 10^7\ M^{-1}$, ([EB] = 4.0 µM). The K_{app} value is 5.20×10^5, 2.68×10^5 and $7.05 \times 10^5\ M^{-1}$ for **1**, **2**

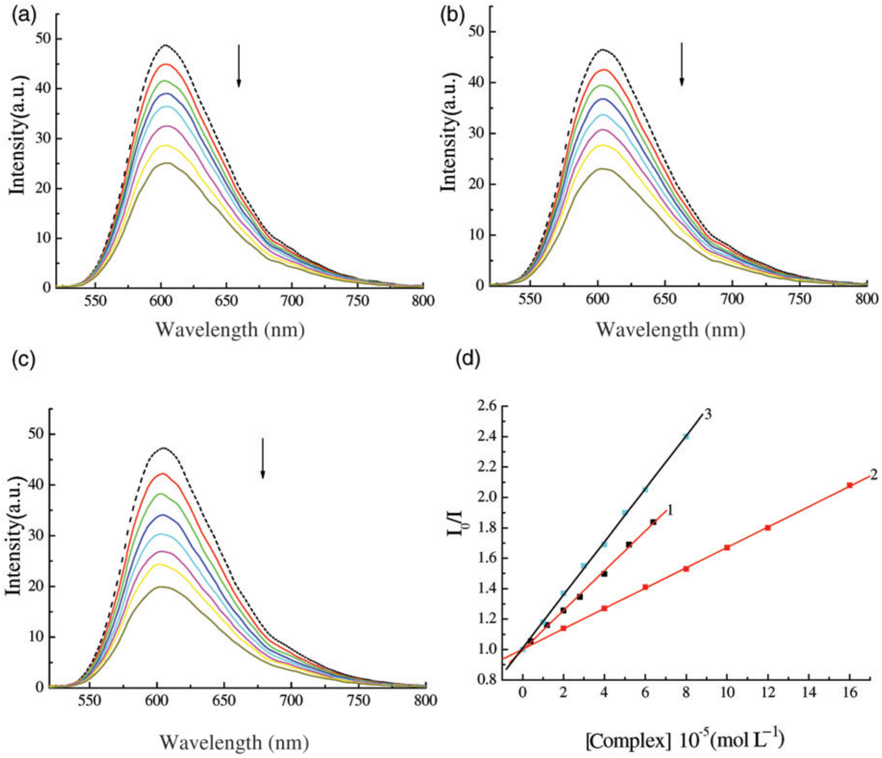

Figure 3. Fluorescence quenching curves of EB bound to DNA by **1** (a), **2** (b) and **3** (c). Figure 3d Plot of I_0/I *vs.* [complex]. $\lambda_{ex} = 510$ nm.

and **3**, less than the binding constant of classical intercalators and metallointercalators (10^7 M^{-1}) [45], suggesting that the interactions of **1**–**3** with DNA are moderate intercalative modes.

3.5. *pBR322 DNA cleavage by the copper(II) complexes*

The chemical nuclease activities of the complexes have been studied using supercoiled pBR322 plasmid DNA in 50 mM *Tris*-HCl/NaCl buffer (pH = 7.2) in the absence of reducing agent under physiological conditions. When circular plasmid DNA is conducted by electrophoresis, the fastest migration will be observed for the supercoiled form (Form I). If one strand is cleaved, the supercoils will relax to produce a slower-moving nicked circular form (Form II). If both strands are cleaved, a linear form (Form III) will be generated that migrates between Form I and Form II. Figure 4 shows the results of gel electrophoretic separations of plasmid pBR322 DNA induced by increasing concentration of complexes in the absence of reducing agent. With increase of complex concentration, Form I plasmid DNA is gradually converted into Form II (lanes 1–5). In addition, a time course of a gel electrophoresis pattern of pBR322 DNA cleavage during a reaction in the presence of 100 µM complex at pH = 7.2 and 37°C is shown in the Supplementary material. With increase in the reaction time, the amount of Form II increased and Form I gradually disappeared. After 180 min (lane 6) linear

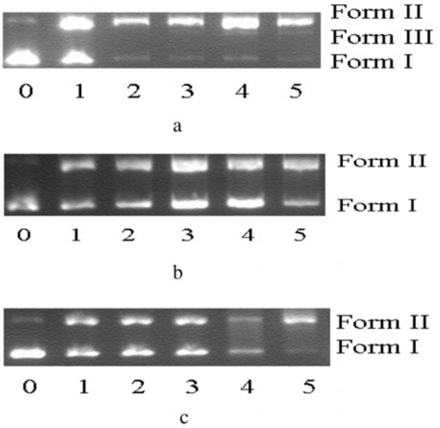

Figure 4. Agarose gel electrophoresis of pBR322 plasmid DNA treated with complexes in the absence of reducing agents at different concentrations. Lane 0: supercoiled DNA (control); lane 1–5: (a) **1**: 10, 100, 200, 300, 400 µM, (b) **2**: 100, 250, 400, 600, 800 µM, (c) **3**: 100, 250, 400, 600, 800 µM.

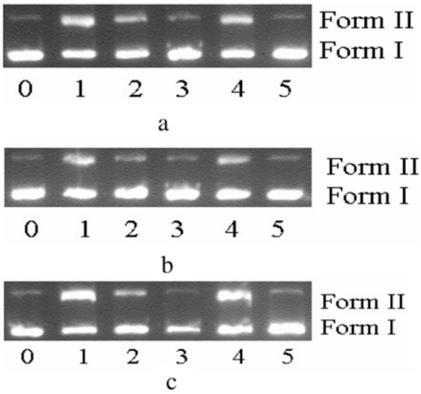

Figure 5. Agarose gel electrophoresis of pBR322 plasmid DNA treated with 100 µM complexes (in the absence of reducing agents) in presence of potential inhibitor agents (a, complex **1**; b, complex **2**; c, complex **3**). Incubation time 3 h (37°C). Lane 0: supercoiled DNA (control); lane 1: complexes; lane 2: complexes + DMSO (1 M); lane 3: complexes + NaN_3 (100 Mm), lane 4 : complexes + SOD (15 units) ; lane 5 : complexes + EDTA (1 Mm).

DNA (Form III) was observed for **1**, however, no Form III appeared for **2** and **3**. Thus, compound **1** more effectively cleaves the pBR322 plasmid DNA than **2** and **3** without addition of external agents; cleavage of DNA by the complexes is dependent on concentration of complex and reaction time. That **1** exhibits enhanced reactivity with supercoiled plasmid DNA suggests a possible synergy between the two copper ions in **1** that contributes to its nucleolytic efficiency. Additionally, increases in the electrostatic attraction of the dicopper complex for DNA relative to the mononuclear copper complexes **2** and **3** may enhance reactivity.

The DNA cleavage mechanisms of the complexes were investigated in the presence of a hydroxyl radical scavenger (DMSO), a superoxide scavenger (SOD), a singlet oxygen quencher (NaN_3) and a chelating agent (EDTA) [46] under physiological conditions (figure 5, lanes 2–6). The SOD enzyme had no effect on the cleavage reaction (lane 4), suggesting that the superoxide is not involved in the cleavage process. Azide (lane 3) inhibits DNA cleavage indicating that $^1O_2$ is involved in the reaction. The hydroxyl radical scavenger, DMSO (lane 2), diminishes significantly the nuclease activity indicative of involvement of the hydroxyl radical in the cleavage process. In order to further clarify the cleavage mechanism of pBR322 DNA induced by complexes, it is necessary to perform the cleavage experiment under anaerobic conditions, as shown in Supplementary material, lanes 0–8; the results show that the complexes hardly cleave pBR322 plasmid DNA under anaerobic conditions. We hypothesize that the copper(II) complexes examined here promote DNA cleavage through an oxidative DNA damage pathway, in which the active oxygen species involved in the reaction are singlet oxygen ($^1O_2$) and hydroxyl radical (OH).

4. Conclusions

We have synthesized and characterized one dimeric dichloro-bridged (**1**) and two mononuclear (**2**, **3**) Cu^{II} complexes of 1,10-phenanthroline-5,6-dione. The complexes cleave plasmid DNA without addition of external agents at $pH = 7.2$ and 37°C and **1** is most effective. DNA cleavage mechanism studies show that complexes promote DNA cleavage through an oxidative DNA damage pathway. The greater efficiency of binuclear complex relative to mononuclear is consistent with their relative abilities to activate dioxygen.

Supplementary material

Crystallographic data for the structural analysis have been deposited with the Cambridge Crystallographic Data Centre with CCDC-680013 (complex **1**). Copy of the data can be obtained free of charge on application to CCDC, Email: deposit@ccdc.cam.ac.uk or http://www.ccdc.cam.ac.uk).

Acknowledgment

This work was supported by the National Natural Science Foundation of China (No. 20771063).

References

[1] D.M. Perrin, A. Mazumder, D.S. Sigman. In *Progress in Nucleic Acid Chemistry and Molecular Biology*, W. Cohn, K. Moldave (Eds), Vol. 52, p. 123, AcademicPress, New York (1996).
[2] G. Pratviel, J. Bernardou, B. Meunier. *Angew. Chem. Int. Ed. Engl.*, **34**, 746 (1995).
[3] G. Pratviel, J. Bernardou, B. Meunier. *Adv. Inorg. Chem.*, **45**, 251 (1998).
[4] J.L. Garcia-Gimenez, G. Alzuet, M.G. Alvarez, A. Castineiras, M. Liu-Gonzalez, J. Borras. *Inorg. Chem.*, **46**, 7178 (2007).

[5] D.S. Sigman, D.R. Graham, V. D'Aurora, A.M. Stern. *J. Biol. Chem.*, **254**, 12269 (1979).
[6] D.S. Sigman, A. Mazumder, D.M. Perrin. *Chem. Rev.*, **93**, 2295 (1993).
[7] D.S. Sigman, T.W. Bruce, A. Mazumder, C.L. Sutton. *Acc. Chem. Res.*, **26**, 98 (1993).
[8] E.K. Efthimiadou, M.E. Katsarou, A. Karaliota, G. Psomas. *J. Inorg. Biochem.*, **102**, 910 (2008).
[9] C.J. Burrows, J.G. Muller. *Chem. Rev.*, **98**, 1109 (1998).
[10] A. Spassky, D.S. Sigman. *Biochemistry*, **24**, 8050 (1985).
[11] B.P. Hudson, J.K. Barton. *J. Am. Chem. Soc.*, **120**, 6877 (1998).
[12] D.S. Sigman. *Biochemistry*, **29**, 9097 (1990).
[13] M.M. Meijler, O. Zelenko, D.S. Sigman. *J. Am. Chem. Soc.*, **119**, 1135 (1997).
[14] S.A. Ross, M. Pitie, B. Meunier. *Eur. J. Inorg. Chem.*, **3**, 557 (1999).
[15] C.H.B. Chen, L. Miline, R. Landgraf, D.M. Perrin, D.S. Sigman. *Chem. Biochem.*, **2**, 735 (2001).
[16] T.B. Thederahn, M.D. Kuwabara, T.A. Larsen, D.S. Sigman. *J. Am. Chem. Soc.*, **111**, 4941 (1989).
[17] S. Ferrer, R. Ballesteros, A. Sambartolom, M. Gonzalez, G. Alzuet, J. Borras, M. Liu. *J. Inorg. Biochem.*, **98**, 1436 (2004).
[18] Q. Jiang, N. Xiao, P.F. Shi, Y.G. Zhu, Z.J. Gou. *Coord. Chem. Rev.*, **251**, 1951 (2007).
[19] B.C. Bales, M. Pitie, B. Meunier, M.M. Greenberg. *J. Am. Chem. Soc.*, **124**, 9062 (2002).
[20] L.P. Lu, M.L. Zhu, P. Yang. *J. Inorg. Biochem.*, **95**, 31 (2003).
[21] E.L. Hegg, J.N. Burstyn. *Coord. Chem. Rev.*, **173**, 133 (1998).
[22] K.J. Humphreys, K.D. Karlin, S.E. Rokita. *J. Am. Chem. Soc.*, **124**, 6009 (2002).
[23] M.G. Alvarez, G. Alzuet, J. Borras, M. Pitie, B. Menier. *J. Biol. Inorg. Chem.*, **8**, 644 (2003).
[24] J.K. Barton, I. Bertini, H.B. Gray, S.J. Lippard, J.S. Valentine (Eds). *Bioinorganic Chemistry*, p. 455, University Press, Mill Valley, CA (1994).
[25] C.G. Pierpont. *Coord. Chem. Rev.*, **216–217**, 99 (2001).
[26] C. Pierpont, C.W. Lange. *Prog. Inorg. Chem.*, **41**, 331 (1994).
[27] C.G. Pierpont, R.M. Buchanan. *Coord. Chem. Rev.*, **38**, 45 (1981).
[28] T. Fujihara, R. Okamura, T. Wada, K. Tanaka. *J. Chem. Soc., Dalton Trans.*, 3221 (2003).
[29] Y.Y. Kou, G.J. Xu, W. Gu, S.P. Yan. *J. Coord. Chem.*, **61**, 3147 (2008).
[30] M. Yamada, Y. Tanaka, Y. Yoshimoto, S. Kuroda, I. Shimao. *Bull. Chem. Soc. Jpn*, **65**, 1006 (1992).
[31] G.M. Sheldrick. *Correction Software*, University of Gottingen, Germany (1996).
[32] G.M. Sheldrick. *SHELXS- 97, Program for the Solution of Crystal Structures*, University of Gottingen, Germany (1997).
[33] G.M. Sheldrick. *SHELXL-97, Program for the Refinement of Crystal Structures*, University of Gottingen, Germany (1997).
[34] J. Marmur. *J. Mol. Biol.*, **3**, 585 (1961).
[35] M.E. Reichmann, S.A. Rice, C.A. Thomas, P. Doty. *J. Am. Chem. Soc.*, **76**, 3047 (1954).
[36] R.P. Herzberg, P.P. Derwan. *J. Am. Chem. Soc.*, **104**, 313 (1982).
[37] C.K. Mirabelli, C.H. Huang, S.T. Crooke. *Cancer Res.*, **40**, 4173 (1980).
[38] C.A. Detmer, F.V. Pamatong, J.R. Borcarsly. *Inorg. Chem.*, **35**, 6292 (1996).
[39] A.W. Addison, T.N. Rao. *J. Chem. Soc., Dalton Trans.*, 1349 (1984).
[40] M.D. Stephenson, M.J. Hardie. *J. Chem. Soc., Dalton Trans.*, 3407 (2006).
[41] M. Rodríguez, A. Llobet, M. Corbella, A.E. Martell, J. Reibenspies. *Inorg. Chem.*, **38**, 2328 (1999).
[42] X.H. Bu, M. Du, L. Zhang, Z.L. Shang, R.H. Zhang, M. Shionoya. *J. Chem. Soc., Dalton Trans.*, 729 (2001).
[43] M. Du, Y.M. Guo, X.H. Bu, J. Ribasb, M. Monfort. *New J. Chem.*, **26**, 645 (2002).
[44] W.E. Marsh, W.E. Hatfield, D.J. Hodson. *Inorg. Chem.*, **21**, 2679 (1982).
[45] V.A. Bloomfield, D.M. Crothers, I. Tinocco Jr.. *Physical Chemistry of Nucleis Acids*, p. 432, Harper & Row, New York (1974).
[46] S. Mahadevan, M. Palaniandavar. *Inorg. Chem.*, **37**, 693 (1998).
[47] T. Hirohama, Y. Kuranuki, E. Ebina, T. Sugizaki, H. Arii, M. Chikira, P.T. Selvi, M. Palaniandavar. *J. Inorg. Biochem.*, **99**, 1205 (2005).
[48] J.R. Lakowicz, G. Webber. *Biochemistry*, **12**, 4161 (1973).
[49] J. Qian, W. Gu, H. Liu, F.X. Gao, L. Feng, S.P. Yan, D.Z. Liao, P. Cheng. *J. Chem. Soc., Dalton Trans.*, 1060 (2007).
[50] M.G. Alvareza, G. Alzueta, J.L.G. Gimeneza, B. Macıasb, J. Borrasa. *Z. Anorg. Allg. Chem.*, **631**, 2181 (2005).